



**HAL**  
open science

## **Pith location tool and wood diameter estimation: Validity and limits tested on seven taxa to approach the length of the missing radius on archaeological wood and charcoal fragments**

Alexa Dufraisse, Jérémie Bardin, Llorenç Picornell-Gelabert, Sylvie Coubray,  
Maria-Soledad Garcia-Martinez, Michel Lemoine, Silvia Vila Moreiras

### ► **To cite this version:**

Alexa Dufraisse, Jérémie Bardin, Llorenç Picornell-Gelabert, Sylvie Coubray, Maria-Soledad Garcia-Martinez, et al.. Pith location tool and wood diameter estimation: Validity and limits tested on seven taxa to approach the length of the missing radius on archaeological wood and charcoal fragments. *Journal of Archaeological Science: Reports*, 2020, 29, pp.102166. 10.1016/j.jasrep.2019.102166 . mnhn-03008213

**HAL Id: mnhn-03008213**

**<https://mnhn.hal.science/mnhn-03008213>**

Submitted on 16 Nov 2020

**HAL** is a multi-disciplinary open access archive for the deposit and dissemination of scientific research documents, whether they are published or not. The documents may come from teaching and research institutions in France or abroad, or from public or private research centers.

L'archive ouverte pluridisciplinaire **HAL**, est destinée au dépôt et à la diffusion de documents scientifiques de niveau recherche, publiés ou non, émanant des établissements d'enseignement et de recherche français ou étrangers, des laboratoires publics ou privés.

1 **Pith location tool and wood diameter estimation: validity and limits tested on seven taxa**  
2 **to approach the length of the missing radius on archaeological wood and charcoal**  
3 **fragments.**

4  
5  
6  
7 DUFRAISSE, Alexa<sup>1</sup>

8 BARDIN, Jérémie<sup>2</sup>

9 PICORNELL-GELABERT, Llorenç<sup>3</sup>

10 COUBRAY, Sylvie<sup>1,4</sup>

11 GARCIA-MARTINEZ, Maria Soledad<sup>1,5</sup>

12 LEMOINE, Michel<sup>1</sup>

13 VILA MOREIRAS, Silvia<sup>1,6</sup>

14  
15 1. CNRS/ MNHN, UMR 7209 Archéozoologie, Archéobotanique: Sociétés, Pratiques et  
16 Environnements, Sorbonne Université, CP56, 55 rue Buffon, 75005 Paris, France.

17 [alexa.dufraisse@mnhn.fr](mailto:alexa.dufraisse@mnhn.fr). Corresponding author

18 2. Sorbonne Université, MNHN, CNRS, Centre de Recherche en Paléontologie - Paris (CR2P),  
19 4 Place Jussieu, 75005 Paris, France.

20 3. ArqueoUIB Research Group. Department of Historical Sciences and Theory of Arts.  
21 University of the Balearic Islands. Carretera de Valldemossa KM 7, 5, 07122, Palma, Balearic  
22 Islands, Spain.

23 4. INRAP Centre-Ile-de-France, 41 rue Delizy, 93690 Pantin cedex

24 5. Departamento de Prehistoria, Arqueología, Historia Antigua, Historia Medieval y Ciencias  
25 y Técnicas Historiográficas, Facultad de Letras, Universidad de Murcia. C/ Santo Cristo, 1.  
26 30001-Murcia.

27 6. Dpt. de Història. Universitat de Lleida 25003 Lleida, Spain.

28  
29  
30 **Abstract**

31 The study of timber wood and wood charcoal fragments from archaeological sites (aka  
32 anthracology) constitutes a relevant archaeobotanical field of research for both landscape  
33 reconstruction and the study of past people-woodlands interactions. Regarding this second  
34 research field, variables other than taxa are known to be a key to the social organization of  
35 woodland management. In this sense, wood diameter constitutes a core factor of fire  
36 management, fuel provisioning and both firewood and timber procurement. These wood uses  
37 are most commonly represented in the archaeological record by charcoal fragments (both  
38 dispersed in the sediment and/or concentrated in fire structures) due to the fact the wood  
39 experiences both mass loss and fragmentation during carbonization. So the original form of the  
40 wood used (trunk, branch, twig) is no longer recognizable. Different pith-location tools (PLT)  
41 have been proposed previously in order to virtually locate the charcoal fragment in relation to  
42 the central part of the stem or trunk (pith) where the used wood originally came from. Among  
43 them, PLTs based on trigonometry are proven to be the most reliable, but have not yet been

44 extensively tested on referential datasets in order to establish reliable analysis of the accuracy  
45 of the measurement of the missing radius, margins of error and correction factors. In this study  
46 we present an experimental referential dataset for 7 different taxa, both angiosperms and  
47 gymnosperms. The first aim was to move forward on the establishment of the trigonometric  
48 tool by testing if it is also suitable and valid for all the woody species producing tree rings. The  
49 second purpose was to provide a ready-to-use tool to estimate the missing radius with an  
50 interval of confidence. Lastly we also tested the effect of the carbonization on two taxa.  
51 According to the results obtained, a measuring protocol, correction factors and guidelines to  
52 interpret the subsequent results are established. In addition, an R function is now available to  
53 estimate the real radius from the calculated one with PLTs.

54

55 **Keywords:** wood pith location; referential datasets; software; dendro-anthracology; wood  
56 diameter estimation; firewood and timber exploitation

57

58

## 59 **Introduction**

60

61 Wood diameter constitutes a social selection criterion as relevant as species, whether to manage  
62 a fire according to the uses of the hearth or to select timber for construction or woodworking as  
63 shown by diverse ethnoarchaeological studies (Zapata Peña et al., 2003; Dufraisse et al., 2007;  
64 Picornell-Gelabert et al., 2011). The carbonized and fragmented residues of this use of wood as  
65 firewood or timber are most often preserved in the archaeological record (charcoal fragments  
66 dispersed on the sediments and/or concentrated in fire structures, such as hearth and ovens).  
67 Wood experiments both mass loss and fragmentation during carbonization, so the original form  
68 of the wood used (trunk, branch, twig) is no longer recognizable. This fact makes it difficult to  
69 archaeologically evaluate the role of the wood diameter as a selective criteria of wood uses and  
70 woodlands management by past human societies.

71 In recent years, new measurement techniques have been developed in order to estimate the  
72 diameter of the wood from which the archaeological charcoal fragments originates. One of the  
73 main research fields in this sense is the establishment of reliable techniques to measure the  
74 distance between the preserved archaeological charcoal fragment and the pith of the  
75 trunk/branch where the fragment comes from. This measurement technique consists of virtually  
76 positioning a charcoal fragment in relation to the central part of the stem or trunk (pith), which  
77 is missing in most of the cases (pith-location tool, PLT). This measurement constitutes a

78 necessary first step to latter estimate the original diameter of the wood exploited in the past  
79 (Dufraisse and Garcia-Martinez, 2011).

80 Different “naked-eye” methods guided by a printed graduated target and based on tree-ring  
81 boundary’ morphology (ring curvature) were proposed to estimate the length of the missing  
82 radius (Applequist, 1958; Willerding, 1971; Lundström-Baudais, 1986; Ludemann and Nelle,  
83 2002; Rozas, 2003; Dufraisse, 2005; Marguerie and Hunot 2007).

84 Later on, experimental research was set up to evaluate two techniques of measurement using  
85 image-analysis software. The “circle tool technique” is one of them, initially proposed by J.  
86 Chrzavzez (2006) and based on the curvature of tree-ring boundaries. Another tool tested, the  
87 “trigonometric tool”, is based on the measurement of angles and distance between ligneous  
88 rays, proposed by A. Dufraisse and developed together with S. Paradis-Grenouillet and M.S.  
89 Garcia-Martinez (Paradis-Grenouillet et al., 2013; Dufraisse and Garcia-Martinez, 2011). These  
90 studies were developed on different taxa, *Quercus petraea*, *Pinus halepensis* and *Fagus*  
91 *sylvatica*. They showed that measurements of the radius of curvature based only on the  
92 curvature of the tree-ring boundaries must be avoided due to the fact that calculated missing  
93 radius did not correspond to the real radius.

94

95 On the contrary, the estimation of the missing radius on the 3 taxa tested (*Quercus petraea*,  
96 *Fagus sylvatica* and *Pinus halpensis*) with the trigonometric tool (angle and distance between  
97 ligneous rays) in a right-angled triangle provides relevant results:

98 *i)* Strong correlation exists between the exact value of the length of the missing radius (real  
99 radius, RR) and its measurement (calculated radius, CR);

100 *ii)* Other trigonometric techniques, such as Thales’ theorem and trigonometry in an isosceles  
101 triangle, provide similar results (Paradis-Grenouillet et al., 2013).

102

103 Building on this previous research, the aim of this study is to move forward on the establishment  
104 of the trigonometric tool by testing if it is also suitable and valid for all the woody species  
105 producing tree rings and to provide a ready-to-use tool to estimate the missing radius with an  
106 interval of confidence. To do so we establish an empirical reference dataset for seven different  
107 taxa with different wood anatomy (both conifers and angiosperms) and commonly identified in  
108 archaeological charcoal spectra in Europe. We later compare the relative errors between species  
109 according to 1) the angle and the distance between the two ligneous rays 2) and the diameters.

110

111 As the Pith Location Tool (PLT) is mainly applied to wood charcoal fragments, we also  
112 investigate the effect of the carbonization, which induces deformation (distortion of shape and  
113 shrinkage), on the efficiency in evaluating the missing radius with the PLTs.

114  
115

## 116 **Materials and methods**

117 The referential dataset was developed in the framework of the DENDRAC project  
118 “Development of DENDRometrical tools used in anthrACology: study of the interactions  
119 between man, resources and environments” funded by the French National Agency of Research  
120 (<http://dendrac.mnhn.fr/>). This program follows key experimental principles to allow relevant  
121 subsequent comparisons of the data obtained, mainly the use of common protocols for all the  
122 different taxa and a restricted number of operators.

123

### 124 *Measurement tools and materials*

125

126 All the measurements were performed using the NIS Element image-analysis software  
127 developed by Nikon. The NIS Elements software was associated to a Nikon camera assembled  
128 to a multizoom microscopes (Nikon AZ100) with objectives covering a diverse range of  
129 magnifications (from x5 to x400) and to a binocular stereo microscope (Nikon SMZ 745, x6 to  
130 x50). Different PLTs based on trigonometric principles were tested. They are all based on the  
131 acquisition of two measures at the same ring boundary: 1) the angle between two ligneous rays  
132 and 2) the distance between the same two ligneous rays. These measurements allow estimating  
133 the length of the missing radius (this is, the distance between the ring boundary measured and  
134 the missing pith).

135

136 The first PLT is a manual one, based on the trigonometry in a right-angled triangle and  
137 involving 12 landmarks fixed by using the NIS element software. The measurements were  
138 carried out under a binocular stereoscope with x10 magnification and a measurement field of  
139 L0,84 cm x h0,63 cm, compatible with small fragments often found in archaeological charcoal  
140 assemblages.

141

142 The second PLT is a semi-automatic method based on 4 landmarks, which is less time-  
143 consuming and more adapted to a routine use. Based on the trigonometry in an isosceles  
144 triangle, it was tested under the multizoom microscope with an objective of x0.5 magnification

145 and digital zoom (e.g. measurement field dimensions with the lowest magnification: L 2,2 cm  
146 x h1,7 cm).

147

148 The two PLTs (manual and semi-automatic) were tested on perfect targets printed on white  
149 paper. The referential based on fresh and carbonized wood slices was realised with the manual  
150 PLT and completed with the semi-automatic PLT.

151

152 - Perfect target

153 The PLTs were first calibrated on perfect targets with a range of radius between 0.5 cm and  
154 17.5 cm (i.e. range of diameter : 1;2;3;5;10;12;15;18;20;25;30;35 cm) and angles between 2  
155 and 70°.

156 For each method of measurement (manual and semi-automatic), from 25 to 30 measures were  
157 carried out according to radius and angles, e.g. 1320 measures / method and 2640 measurements  
158 in total (Table 1). In some cases (see \* in Table 1), measurements could not have be taken due  
159 to either the dimension of the measurement field or printing problems with the target especially  
160 between 0.5 and 1 cm of radius and small angles (2° and 4°).

161

162 - Fresh wood

163 Seven taxa with different anatomical characteristics (Angiospermae vs Gymnospermae,  
164 presence of uniseriate and/or multiseriate rays, ring porous/diffuse wood, etc.) were studied:  
165 Gymnosperm: *Pinus halepensis* (uniseriate rays); ring porous Angiosperms: *Quercus petraea*  
166 (uni- and multiseriate rays), *Castanea sativa* (uniseriate rays), *Fraxinus excelsior* (2-3 seriate  
167 rays), *Ulmus minor* (3-5 seriate rays); diffuse porous Angiosperms: *Fagus sylvatica*  
168 (multiseriate), *Prunus avium* (3-5 seriate rays). As far as it was possible, from one to six wood  
169 slices from different trees coming from different locations were analysed for every taxon to  
170 record a maximum of variability (excepted for *Ulmus*, *Prunus* and *Castanea*). Measurements  
171 were performed on fresh wood slices after a fine sanding of the surface. A total of 4164  
172 measures were carried out (see the total number of measurements in Table 2).

173

174 - Carbonized wood

175 In order to evaluate the PLT on carbonized wood slices, we measured before and after  
176 carbonization two of the studied taxa: *Pinus halepensis* and *Fagus sylvatica* (Table 2). Two  
177 wood slices for *Pinus* (R1, R2) and one for *Fagus* (R13) were carbonized in a muffle furnace  
178 at 300°C during two hours according to its thickness. The measured shrinkage fluctuates from

179 14.7% (slice R2, 14,5 x 13 cm) to 15.38% (slice R1, 16,5x 16,4 cm) and is about 20% on *Fagus*  
180 *sylvatica* (R13). In total, 720 measures were carried out on this carbonized material (Table 2).

181

### 182 *Data Treatment*

183

184 The PLT we provide consists in producing an estimation of the real radius (RR) given the  
185 calculated radius (CR). For each measure, we registered the real radius (RR), the angle and the  
186 distance between the two rays, and the calculated radius by using the trigonometric tool (CR).

187 The relative error (RE) was calculated following the equation:  $RE = (CR - RR) * 100 / RR$ . Some  
188 values of RE are negative due to possible underestimations of CR. In order to have a comparable  
189 measure of error (i.e. both negative and positive), we used the Absolute Relative Error:  $ARE =$   
190  $(|CR - RR|) * 100 / RR$ .

191

192 While most of the observations follow a straight regression line, for small angles, CR and thus  
193 ER show obvious outliers. We tried several methods to identify and remove them in order to  
194 provide the user a practical minimum angle (see SM1). Unfortunately, none of these methods  
195 allowed us to identify a clear angle limit from which all observations could be included. As we  
196 want to perform the regressions on every observations starting from a given angle to include  
197 the whole variation of the selected range, we chose 2° as the lower limit, a solution which is  
198 reproducible on archaeological charcoal assemblages.

199

200 In order to understand the relation between RR and CR, we use our dataset as a training sample  
201 in order to establish models suited to estimate the RR on archaeological wood / charcoal  
202 fragments based from the CR by using the provided PLT. An eye-check on a bivariate  
203 representation of RR over CR (see Fig. 3 in Results) strongly suggests that the relationship  
204 between these two variables is linear. We therefore try to model this relationship with a linear  
205 model with RR as the response variable and CR as the explanatory variable (*reg*). The variance  
206 of RR increases over the range of CR. To take this into account, we performed a weighted  
207 regression with the weights of each observation being  $1/CR$  (*wreg*). Secondly, we noticed that  
208 the relationship between RR and CR may be piecewise, with a potential important decrease of  
209 the slope for highest values of CR (see Fig. 4 in Results). To investigate this issue, we fit a  
210 regression model for each species with broken line relationships (*swreg* = segmented weight  
211 regression model) using the R package *segmented* (Muggeo, 2008). This model can be viewed  
212 as a linear regression from which we allow the relationships between CR and RR (i.e the slope)

213 to change on each side of a breakpoint represented by the parameter  $\alpha$ . Using such a model is  
214 of prime importance as the relationship seems stronger for low values of CR. This allows us to  
215 test precisely each part of the relationship and to locate on which of those part the prediction  
216 are the best. AIC (Akaike, 1973) allows finding the adequate balance between the goodness of  
217 fit and the number of parameters. We use it to select the best model for each species (i.e. reg,  
218 wreg, swreg; Table 3).

219  
220

221 To investigate the effect of carbonization on the relationship between CR and RR, we add to  
222 the model swreg an additional discrete variable representing the carbonization (here after called  
223 *swregCarb*). We use the approach proposed by Muggeo (2008) to split the values of the  
224 explanatory variable (i.e. CR) for the different levels of the factor (i.e. carbonized or not).

225

## 226 **Results**

### 227 *Comparison of manual and semi-automatic PLTs on perfect target*

228

229 The analysis of the manual PLT on perfect target is based on 1320 measurements. The mean of  
230 the Absolute Relative Error (ARE) and its standard error is  $3.52\% \pm 0.48$ . The correlation of  
231 the exact and the approximated value of the radius is 0.9953078 (method = Spearman, p-value  
232  $< 2.2e-16$ ).

233 The test of the semi-automatic PLT is also based on 1320 measurements. The mean of ARE  
234 and its standard error is  $2.44\% \pm 0.3$ . The correlation of the exact radius and the approximated  
235 radius is 0.9958947 (method = Spearman, p-value  $< 2.2e-16$ ).

236 A Wilcoxon-Mann-Whitney test between RE from the manual and the semi-automatic PLT  
237 indicates a significantly different median. However, the differences are very fine as shown by  
238 Figure 1. Indeed, the manual PLT has a slightly negative ER when semi-automatic PLT is  
239 centred on zero. Then, the semi-automatic PLT works slightly better than the manual PLT.

240

### 241 *Establishment of exclusive criteria*

242

243

244 The analysis of the distribution of the Relative Error (RE) on perfect targets, according to angle  
245 and distance, indicates that the distribution of RE decrease obviously from angles bigger than  
246  $10^\circ$ . The biggest RE is reached for the smallest angle ( $2^\circ$ , ARE = 5.27%, sd= 4.39%) (Fig. 2).  
247 The analysis of RE values according to RR indicates that there is no correlation between these  
248 two parameters (Pearson correlation coefficient = 0.009, p-value = 0.5).

249

250 Thus, exclusive criteria to avoid inexact measurements using the PLT on archaeological  
251 charcoal fragments have been established according to the analysis of the referential dataset.

252 Indeed, for all taxa together (fresh wood), and all angles and distances included, the mean of  
253 the ARE and its standard deviation are  $0.511 \pm 5.47$ .

254 The analysis of the RE according to distance and angle indicates that the most important RE  
255 concerns angle below  $2^\circ$  (Fig. 2, SM2). Most often, these small angles correspond to small  
256 distances between rays, less than 2 mm. Integrating these exclusive criteria, the mean of the  
257 ARE and its standard deviation are  $0.25 \pm 0.24$ . The correlation between the exact values of  
258 radius and its approximate values is 0.8832283 (method = Spearman, p-value  $< 2.2e-16$ ). The  
259 following analyses presented include the exclusive criteria.

260

261

262 *Comparison between taxa (fresh wood) and modeling of the relation between RR and CR*

263

264

265 The bivariate representation of RR over CR (Fig.3) from data measured on fresh wood strongly  
266 suggests that the relationship between these two variables is linear. However, the variance of  
267 RR increases over the range of CR.

268 A comparison of the results obtained with the referential analysis was performed in order to  
269 compare the results of the PLT on the different taxa and to model the relation between the RR  
270 and the CR (Table 4, data treatment). Thus, a regression model for each species with broken  
271 line relationships was performed (Fig. 4, Table 4).

272

273 The first slopes (lowest CR) are very similar between taxa excepted for *Pinus halepensis*.  
274 Indeed, very low CR values corresponding to a wide range of RR values are to be noted without  
275 explanation (Fig. 3, *Pinus halepensis*).

276 Thus, the smallest breakpoint concerns *Pinus halepensis* with a CR of 4.071 cm that means  
277 about 8 cm of diameter. Below this breakpoint, the correlation between CR and RR is very  
278 strong while above 4 cm, the estimation of RR from CR is no more reliable, characterized by a  
279 nearly flat regression line.

280 The swreg model indicates also a low breakpoint for *Quercus petraea* as for *Pinus*. However,  
281 after this breakpoint, CR is still correlated with RR even if the interval of confidence is large.

282

283 At the opposite, the highest breakpoint corresponds to *Prunus avium* with a CR = 9.833 cm that  
284 means about 20 cm of diameter. In other words the correlation between CR and RR is very  
285 strong for diameters less than 20 cm while the estimation of RR for largest diameter is no more  
286 reliable, characterized by a downward slope. *Fagus sylvatica* presents similar behavior.

287

288 Lastly, *Ulmus minor*, *Fraxinus excelsior* and *Castanea sativa* are between these two groups  
289 with a breakpoint at CR = 5.475, CR = 6.958 and CR = 6.043, respectively. Before the  
290 breakpoint, the correlation between RR and CR is very strong. After it, the correlation is less  
291 accurate but still reliable despite a large interval confidence (the signal is preserved).

292

### 293 *Effects of carbonization*

294 In order to evaluate the efficiency of the PLTs on carbonized wood, we repeated the same  
295 protocols on carbonized slices for *Pinus halepensis* and *Fagus sylvatica*. (Fig. 5, Table 5). To  
296 carry out this comparative analysis, we considered only measurements from fresh wood slices  
297 that were charred (i.e. R1 and R2 for *Pinus*, and R13 for *Fagus*).

298

299 The effect of carbonization is almost negligible on *Pinus sylvestris*. The breakpoint value is  
300 small before carbonization (CR = 4.168 cm). It slightly increases after carbonization (CR =  
301 4.91). In fact, the above-mentioned marginal measures are no longer recorded on carbonized  
302 slices, which is the reason why the slope 1 of carbonized wood is slightly less inclined and the  
303 breakpoint slightly higher. After carbonization, it is interesting to note that the slope 2 is slightly  
304 less flat.

305 On the contrary, the carbonization induces significant changes in the RR estimation for *Fagus*  
306 *sylvatica* whose breakpoint value was high before carbonization (CR = 7.717 cm) and smaller  
307 after carbonization (CR = 4.717 cm). Nevertheless, the slope 1 and the slope 2 before and after  
308 carbonization are very similar. That means the signal is preserved.

309

## 310 **Interpretation and Discussion**

### 311 *PLTs on perfect targets*

312 A manual technique with 12 landmarks and a semi-automatic technique with 4 landmarks (less  
313 time consuming and more suitable for a routine use) using the trigonometric principle were  
314 compared on perfect target printed on white paper. The 1320x2 measures developed show quite  
315 comparable results even if the statistical test indicates a median significantly different. A  
316 previous study showed that Thales' theorem, trigonometry in a right-angled triangle, and

317 trigonometry in an isosceles triangle provide relevant and similar results. They are just more or  
318 less adapted to the software used (Paradis-Grenouillet et al., 2013). Two reasons can be given  
319 to explain why the semi-automatic PLT works slightly better than the manual one. The first one  
320 is the observation equipment. The manual PLT was associated to a binocular stereoscope that  
321 is not recommended in morphometry. The second one is the smaller number of landmarks for  
322 the semi-automatic PLT (4 landmarks instead of 12 for the manual PLT). Indeed, the recorded  
323 relative errors on perfect target are related to handling, i.e. to the operator. Then, the smaller  
324 the number of landmarks is, the less the margins of error are important.

325

### 326 *PLTs on fresh wood*

327 The values of relative errors on fresh wood slices are significantly higher than on perfect targets.  
328 This means that the larger relative errors on fresh wood are related to the anatomy of the wood,  
329 as the RE linked to the operator is marginal. It is impossible to escape this margin of uncertainty,  
330 which is intrinsic to any living phenomenon, as each characteristic of an organism results from  
331 the interaction between its genome and the environment, which is itself greatly variable.

332 In order to limit the margins of error, an exclusive criterion could be set up for the  
333 archaeological application of the PLT: avoid angles  $< 2^\circ$ . In addition, whichever the taxon, RE  
334 values increase significantly in relation to the distance from the pith. Observations of the wood  
335 slices suggest that this is due to the fact that new ligneous rays are inserted during growth of  
336 the stem, the latter not necessarily converging at the level of the pith. In addition, when tension  
337 wood occurs during growth, the direction of the rays can change to adapt to the new wood  
338 morphology. Also, the observation scale, often limited to a camera field about 1 cm<sup>2</sup>, does not  
339 allow to assess local deformations or wood rays which can also be a source of error (Fig. 6 ).

340

### 341 *Comparison between taxa*

342 The variance of RR estimations on fresh wood increases for all taxa over the range of CR. The  
343 segmented weighted regression model allows comparing different taxa. The slope 1, before the  
344 breakpoint, is very similar for all taxa excepted for *Pinus halepensis* due to marginal values.

345 Then, the model indicates similarities between taxa. For example, *Fagus* and *Prunus*, whose  
346 anatomy is very close, are characterized by a high breakpoint (about 10 cm in radius). However,  
347 after this breakpoint, the signal is lost (see slope 2). These two species are diffuse porous wood  
348 with multiseriate rays. Thus, deformation linked to large vessels in earlywood, as it can be seen  
349 in porous wood, is probably limited.

350

351 Other similarities can be observed between *Fraxinus*, *Castanea* and *Ulmus*, whose anatomy is  
352 also close. Their breakpoint ranges from 5.4 cm to 6.9 cm. The signal is well preserved after it  
353 for *Fraxinus*, which is less obvious for *Castanea* and *Ulmus* (see slope 2).

354 Another group is formed by *Pinus* and *Quercus*. They are both characterized by a small  
355 breakpoint (about 4 cm in radius). Nevertheless, the signal is better preserved after this  
356 breakpoint for *Quercus* than for *Pinus*, even if their anatomy is significantly different.

357

358 According to these results, wood anatomy, especially the ligneous rays and probably their  
359 formation, may be an explanation of such variations. However, surprisingly, our understanding  
360 of how wood develops, especially wood rays, is far from complete (for a review, see Lev-  
361 Yadun and Aloni, 1995). Short radial initials (cells in the cambium) give rise to rays that are  
362 essential to the translocation of nutrients between phloem and xylem. As for other wood  
363 elements such as vessels, the cellular and molecular processes are controlled by a wide variety  
364 of factors both exogenous (photoperiod and temperature) and endogenous (phytohormones) and  
365 by interaction between them (Plomion et al., 2001). According to Lev-Yadun and Aloni  
366 (1995), a basic aspect of maturation in woody plants is the normal gradual increase in ray size  
367 with age, with distance from the pith, and with distance from the young leaves. However, the  
368 increase in size and number of rays is not necessarily dependent on the distance between rays.  
369 The greater number of rays generally observed in branches, as compared with the stem, no  
370 doubt correlates with the reduced width of the rings and the associated reduction in caliber of  
371 the tracheids. In *Fraxinus excelsior* and *Castanea sativa* there were more rays per unit area in  
372 the wood with wide growth rings than there were in the slower-growth wood. Concerning *Pinus*  
373 *halepensis*, there is no clear, general conclusion that the rate of cambial activity determines the  
374 number of rays. Lev-Yadun and Aloni (1995) concludes that the rate of cambial activity is not  
375 the only regulating mechanism of ray characteristics, and another explanation for the regulation  
376 of ray formation during cambial activity is needed.

377

### 378 *Effect of carbonization*

379 The results indicate that the effect of the carbonization is different depending on the two taxa.  
380 It is almost negligible on *Pinus*, while on *Fagus* we can observe an obvious decrease of the  
381 breakpoint. The slope 1 is very similar before and after carbonization for the both taxa. After  
382 the breakpoint, the slope 2 indicates that the signal is not well preserved. However, the  
383 reference data is still limited and have to be completed. Xue et al. (2018) analysed the effect of

384 wood rays on the shrinkage of wood during the drying process. The wood is characterized by  
385 an anisotropic shrinkage (as well as during the carbonization): the longitudinal shrinkage from  
386 the green to the dried condition (and during carbonization) is the smallest and the tangential  
387 shrinkage is usually 1.5 to 2.5 times that of radial shrinkage. Their experiments indicate that  
388 the larger the rays, the greater the shrinkage of fibers. In addition, fiber shrinkage is clearly  
389 dependent on the distance from the wood rays. If this study concerns the wood drying process,  
390 it could be assumed that this same process may occur during the carbonization with greater  
391 effects. The most important decreasing of the breakpoint value observed on *Fagus* can thus be  
392 explained by the numerous and multiseriate rays.

393

#### 394 *Measurement protocol*

395

396 Considering the results of this referential study, a measurement protocol can be established in  
397 order to provide a ready-to-use PLT to estimate the missing radius with an interval of  
398 confidence. According to the results, the semi-automatic PLT using a multizoom microscope is  
399 preferred, as it reduces the margins of errors (and measures) and is less time-consuming.  
400 Accordingly, the following protocol is established in order to obtain reliable estimations of the  
401 charcoal-pith distance for archaeological wood and charcoal fragments and to estimate the  
402 original diameter of the wood used:

403

404 1- Each charcoal fragment to measure have to present at least one preserved ring (this is two  
405 ring boundaries) in a transverse section of at least 2 mm length is needed in order to provide a  
406 reliable assemblage to be measured. A limit inherent to the size of archaeological charcoal,  
407 especially for fragments smaller than 4 mm, is noticeable. This limit is directly related to the  
408 minimum angle that must be exceeded to obtain a reliable measurement ( $2^\circ$ ). Thus, the  
409 maximum missing radius that can be measured on transversal section smaller than 4mm\*4 mm  
410 is 11.5 cm (23 cm diameter) (Nocus, 2014).

411

412 2- Orientate each wood/charcoal fragment under the multizoom microscope in order to verify  
413 that the rays are not divergent. Do not measure fragments presenting deformed wood anatomy.  
414 As far as possible, take measurements on the last ring boundary preserved. Eliminate the  
415 measurements with angles  $<2^\circ$ .

416

417 3- Repeat 3 to 5 times the measure on the same ring boundary and with different rays. Discard  
418 the two extreme values (largest and smallest measurements of the missing radius) and calculate  
419 a mean value with the three remaining measures.

420

421 4- An R function and the swreg model with a user guide can be downloaded on the DENDRAC  
422 website in the section Dendro-anthracological tools  
423 (<https://dendrac.mnhn.fr/spip.php?rubrique71>). The function allows to obtain, from the CR, a  
424 RR with margins of error following the model presented in the paper. The result can be  
425 improved considering each taxon independently and/or the state of carbonization. If the taxon  
426 are not referenced in the database, the estimation of RR is given taking into account all the taxa.

427

428 5- If the analysed material is carbonized, correct the shrinkage due to carbonization. At the state  
429 of the art, we assume a mean of 20% in open domestic fireplace. The value can reach 40% in  
430 charcoal kilns. A more precise reference was conducted on *Quercus* and *Castanea* at different  
431 temperatures and taking into account sapwood and heartwood (Paradis-Grenouillet and  
432 Dufraisse, 2018)

433

434 6- (optional) Double the CR final value and locate it into one of the diameter classes proposed  
435 for angiosperms and gymnosperms (this is the actual value that will allow discussing the  
436 composition of the assemblage in relation to diameter). Considering the accuracy of the RR  
437 estimated and the standards used in dendrometrical plans by foresters (Gaudin, 1996; Deleuze  
438 et al., 2014), the values of estimated RR can be ordered into diameter classes as following for  
439 Angiospermae: [0-2] cm, [2-4] cm, [4-7] cm, [7-10] cm, [10-20] and >20 cm; and as following  
440 for Gymnospermae: [0-2] cm, [2-4] cm, [4-7] cm, [7-10] cm, [10-14] cm, [14-20] cm and >20  
441 cm (Dufraisse et al., 2018). However, taking into account the segmented weighted regression  
442 models, data must be interpreted with caution between [10-14] cm, [14-20] cm. It is also  
443 important to note that referential studies for other Gymnospermae should be considered in order  
444 to strength the model for these taxa.

445

446 *Contributions of the use of the trigonometric PLT on archaeological charcoal assemblages.*

447 The PLT has been tested on archaeological charcoal analysis to approach wood management  
448 strategies on different contexts. García-Martínez and Dufraisse (2012) analysed charcoal  
449 fragments at the Argaric Bronze Age site of Barranco de la Viuda, South-Eastern Iberia. In this  
450 case, charcoal-pith distance for diameter restitution has been performed on Aleppo pine (*Pinus*

451 *halepensis*) charcoal fragments from three different assemblages. Small diameters (>10 cm,  
452 mainly 2-5 cm) were exploited to provide firewood for different dwelling and craft activities  
453 performed at the site. The occurrence of saproxylophagous in some of the branches suggested  
454 that firewood provisioning at the site focused on the gathering of Aleppo pine dead branches.

455

456 Aleppo pine charcoal fragments have also been analysed in Late Bronze Age and Iron Age sites  
457 of Mallorca (Balearic Islands, Western Mediterranean, Picornell-Gelabert and Dufraisse 2018).  
458 Assemblages of dispersed charcoal fragments from two different sites abandoned after fire  
459 events were analyzed in order to suggest the original use of pinewood before the firing of the  
460 buildings. At Ses Païsses site the occurrence of diameters >7 cm was minor, while at Son Fornés  
461 site the occurrence was significantly more important. Such results allowed the authors to  
462 suggest that at Son Fornés pine trunks would have been used as constructive material (timber  
463 for beams), while in Ses Païsses Aleppo pine charcoal fragments would mainly represent the  
464 residues of the use of branches as firewood during the occupation of the building before the  
465 final abandonment after the fire event.

466

467 Charcoal-pith distance has been measured on charcoal fragments from historical charcoal kilns  
468 in order to interrogate forest resources management and the exploitation of woody vegetation  
469 to produce energy sources. In this sense, Paradis-Grenouillet et al. (2015) identified the  
470 continuous sustainable exploitation of *Fagus sylvatica* forests at Mont Lozère (France) during  
471 four hundred years (11<sup>th</sup> to 15<sup>th</sup> centuries AD), based on beech coppicing practices by the  
472 Medieval charcoal burners in relation to the metallurgical industry.

473

474 Finally, charcoal-pith distance has been measured on charcoal fragments associated with tree-  
475 ring width and heartwood/sapwood (anthraco-typology) in four Neolithic sites located in  
476 northern France (Houplin-Ancoisne in Deûle's Valley) and Alpine arc (Chalain 4 and Chalain  
477 21 on Lake Chalain, Jura, France) (Coubray and Dufraisse, in press). These tools were  
478 combined with the biological and ecological traits of the woody taxa identified for a systemic  
479 approach to forest space. Two forest management systems are thus detected. The sites on Lake  
480 Chalain are characterized by the exploitation of oak branches, probably from the hinterland,  
481 and ash tree shoots from fragmentary woodland areas. In the Deûle Valley, it is the crown of  
482 trees, such as ash and alder, which were exploited, whereas oak came mainly from the felling  
483 of large trees. These data are integrated coherently into the paleoeconomic syntheses proposed  
484 for these sites, namely, in a mountain context, semi-permanent habitats associated with a

485 shifting agriculture system in the forest where deer hunting played a predominant role, and in  
486 the valley bottom a system of permanent habitats, structured within a densely occupied territory  
487 where the share of livestock was dominant.

488

## 489 **Conclusion and perspectives**

490 The estimation of missing radius (CR, this is the charcoal-pith distance) by using the  
491 trigonometric method, and the constitution of a reference dataset composed of 7 taxa allow  
492 moving forward in the establishment of a reliable and less time-consuming PLT. This study  
493 allows establishing a predictive model and estimating the missing radius and its interval of  
494 confidence. This PLT, thus, allows a rapid and reliable measurement of the charcoal-pith  
495 distance and, subsequently, an estimation of the original diameter up to 20 cm. Beyond this  
496 diameter size, the margins of error detected increase considerably due to the insertion of new  
497 rays during the growing of the tree and the creation of new rings.

498 In this sense, this study shows that carbonization is also a factor to be taken into account to  
499 obtain reliable diameter estimations. In order to solve this, this experimental dataset allows  
500 establishing correction factors of the wood shrinkage during carbonization to be applied to the  
501 CR values obtained with the trigonometric semi-automatic PLT.

502 However, the access to specific equipment (multizoom microscope combined with a software  
503 image analysis) is not always possible due to logistic reasons. We are therefore creating a  
504 printed calibrated target based on the trigonometric principle; this means without taking into  
505 account the tree-ring curvature but based on the angle and the distance between ligneous rays.  
506 The target will be made freely available online (<https://dendrac.mnhn.fr/spip.php?article239>)  
507 and can be printed out on different supports (rigid/soft). This target is ready to use under a  
508 binocular stereomicroscope as a PLT to easily estimate a class of charcoal-pith distance (and  
509 not a strict value) on charcoal fragments big enough.

510

## 511 **Acknowledgements**

512 The authors thank the Agence Nationale de la Recherche (ANR JCJC 200101 DENDRAC, dir.  
513 A. Dufraisse) for financing this study. M.S. Garcia-Martinez's work was financed by the  
514 Fundación Séneca of the Region of Murcia (Spain). The work of Ll. Picornell-Gelabert have  
515 been done thanks to a Juan de la Cierva-Incorporación postdoctoral fellowship of the Spanish  
516 Ministerio de Economía y Competitividad (IJCI-2015-24550). We also thank anonymous  
517 referee for their comments.

518

519

520 **References**

- 521 Akaike, H., 1973. Information Theory and an Extension of the Maximum Likelihood Principle.  
522 In: Petrov, B. N., & Csaki, F. (Eds.), Proceedings of the 2nd International Symposium on  
523 Information Theory. Akademiai Kiado, Budapest, pp. 267-281  
524
- 525 Applequist, M. B., B. 1958. A Simple pith locator for use with off-Center increment cores.  
526 Journal of Forestry 56 (3), 141.  
527
- 528 Chrzavzez, J., 2006. Collecte du bois de feu et paléoenvironnements au Paléolithique. Apport  
529 méthodologique et étude de cas: la grotte de Fumane dans les Pré-Alpes Italiennes. Mémoire  
530 de Master II, Université Paris I, (unpublished).  
531
- 532 Coubray S., Dufraisse A. (2019) - De l'arbre à la forêt domestiquée : pratiques de gestion et  
533 systèmes agroforestiers. Application de l'anthraco-typologie sur des sites néolithiques du Nord  
534 de la France et du pourtour de l'arc alpin, in C. Montoya, J.-P. Fagnart et J.-L. Lochet  
535 (dir.), *Préhistoire de l'Europe du Nord-Ouest. Mobilités, climats et identités culturelles*, actes  
536 du 27<sup>e</sup> congrès préhistorique de France (Amiens, 30 mai-4 juin 2016), vol. 3, Paris, Société  
537 préhistorique française, p. 139-159.  
538
- 539 Deleuze, C., Monreau, F., Renaud, J.P., Vivien, Y., Rivoire, M., Santenoise, Ph., Longuetaud,  
540 F., Mothe, F., Hervé, J.C., Vallet, P., 2014. Estimer le volume total d'un arbre, quelles que  
541 soient l'essence, la taille, la sylviculture, la station. RDV Techniques 44, ONF, pp. 22-32.  
542
- 543 Dufraisse, A., 2005. Economie du bois de feu et sociétés néolithiques. Analyses  
544 anthracologiques appliquées aux sites d'ambiance humide des lacs de Chalain et Clairvaux  
545 (France, Jura). Gallia Préhistoire, 47, 187-233.  
546
- 547 Dufraisse, A., Pétrequin, A. M., Pétrequin, P., 2007. La gestion du bois de feu : un indicateur  
548 des contextes socio-écologiques. Approche ethnoarchéologique dans les Hautes Terres de  
549 Papua (Nouvelle-Guinée indonésienne). In: Besse, M. (Ed.), Sociétés néolithiques. Des faits  
550 archéologiques aux fonctionnements socio-économiques. Actes du 27<sup>e</sup> colloque interrégional  
551 sur le Néolithique (Neuchâtel, octobre 2005). Cahiers d'archéologie romande, Lausanne, vol.  
552 108, pp. 115-126  
553
- 554 Dufraisse, A., Garcia-Martinez, M.S., 2011. Mesurer les diamètres du bois de feu en  
555 anthracologie. Outils dendrométriques et interprétation des données. Anthropobotanica 2, 1-18.  
556
- 557 Dufraisse, A., Coubray, S., Nocus, N., Lemoine, M., Dupouey, J.-L., Marguerie, D., 2018.  
558 Anthraco-typology as a key approach to past firewood exploitation and woodland management  
559 reconstructions. Dendrological reference dataset modelling with dendro-anthracological tools.  
560 Quat. Int. 463 Part B, 232-249. <https://doi.org/10.1016/j.quaint.2017.03.065>  
561  
562
- 563 Garcia-Martinez, M.S., Dufraisse, A., 2012. Correction factors on archaeological wood  
564 diameter estimation. In: Badal E., Carrion Y., Grau E., Macías M., Ntinou M. (Eds), Wood and  
565 charcoal: evidence for human and natural history, Saguntum extra 13, pp. 283-290.  
566
- 567 Gaudin, S., 1996. Dendrométrie des peuplements. BTSA Gestion Forestière, Besançon.  
568

569 Lev-Yadun, S., Aloni, R., 1995. Differentiation of the ray system in woody plants. The  
570 botanical review 61 (1), 45-84  
571

572 Ludemann, T., Nelle, O. (Eds.), 2002. Die Wälder am Schauinsland und ihre Nutzung durche  
573 Bergau und Köhlerei. Fortwissenschaftliche Versuchs- und Forschungsanstalt Baden-  
574 Württemberg, Freiburg.  
575

576 Lundström-Baudais, K., 1986. Etude paléoethnobotanique de la station III de Clairvaux. In:  
577 Pétrequin, P. (Ed.), Les sites littoraux néolithiques de Clairvaux-les-Lacs (Jura). I.  
578 Problématique générale, l'exemple de la station III. Maison des Sciences de l'Homme, Paris,  
579 pp. 311-391.  
580

581 Marguerie, D., Hunot, J.-Y., 2007. Charcoal analysis and dendrology: data from archaeological  
582 sites in western France. J. Archaeol. Sci. 34 (9), 1417-1433.  
583 <https://doi.org/10.1016/j.jas.2006.10.032>  
584

585 Muggeo, V. M. R., 2008. Segmented: an R package to fit regression models with broken-line  
586 relationships. R News 8 (1), 20-25.  
587

588 Nocus, N., 2014. Forêts et Sociétés aux étages planitiaires et collinéens de l'Alsace du  
589 Néolithique au haut Moyen Age : approche dendro-anthracologique. Thèse de doctorat,  
590 Museum national d'histoire naturelle, Paris, (unpublished).  
591

592 Paradis-Grenouillet, S., Dufraisse, A., Allee, P., 2013. Radius of curvature measurements and  
593 wood diameter: a comparison of different image analysis techniques. In: Damblon, F. (Ed.), 4th  
594 International Meeting of Anthracology in Brussels, BAR International Series 2486, pp. 173-  
595 182.  
596

597 Paradis-Grenouillet, S., Allée, Ph., Servera-Vives, G., Ploquin, A., 2015. Sustainable  
598 management of metallurgical forest on Mont Lozère (France) during the Early Middle Ages.  
599 Environ. Archaeol. 20(2), 168-183. <https://doi.org/10.1179/1749631414Y.0000000050>  
600

601 Paradis-Grenouillet, S., Dufraisse, A., 2018. Deciduous oak/chestnut: Differential shrinkage of  
602 wood during charcoalification? Preliminary experimental results and implications for wood  
603 diameter study in anthracology. Quat. Int. 463, 258-267.  
604 <https://doi.org/10.1016/j.quaint.2017.06.074>  
605

606 Picornell-Gelabert Ll., Asouti E., Allué Martí E., 2011. The ethnoarchaeology of firewood  
607 management in the Fang villages of Equatorial Guinea, central Africa: Implications for the  
608 interpretation of wood fuel remains from archaeological sites. J. Anthropol. Archeol. 30, 375-  
609 384. <https://doi.org/10.1016/j.jaa.2011.05.002>  
610

611 Picornell-Gelabert, Ll., Dufraisse, A., 2018. Wood for Building: Woodland Exploitation for  
612 Timber Procurement in the Prehistoric and Protohistoric Balearic Islands (Mallorca and  
613 Menorca; Western Mediterranean). Environ. Archaeol.  
614 <https://doi.org/10.1080/14614103.2018.1521086>  
615

616 Plomion, C., Leprovost G., Stokes, A., 2001. Wood Formation in Trees. Plant Physiology 127,  
617 1513-1523.  
618

619 Rozas, V., 2003. Tree age estimates in *Fagus sylvatica* and *Quercus robur*: testing previous and  
620 improved methods. *Plant Ecology* 167, 193–212.  
621  
622 Willerding, U., 1971. Methodische problem bei der Untersuchung und Auswertung von  
623 Pflanzensenden und frugeschichtlichen Siedlung. *Nachrichten aus Niedersachsens*  
624 *Urgeschichte* 40, 180-188.  
625  
626 Xue, Q., Sun, W., Fagerstedt, K., Guo, X., Dong, M., Wang, W., and Cao, H., 2018. Effects of  
627 wood rays on the shrinkage of wood during the drying process. *BioRes.* 13 (3), 7086-7095.  
628 DOI: 10.15376/biores.13.3.7086-7095  
629  
630 Zapata Peña, L., Pena-Chocarro L., Ibanez Estevez J.J., Gonzalez Urquijo J.E., 2003.  
631 Ethnoarchaeology in the Moroccan Jebala (Western Rif): wood, dung and fuel. In: Neumann,  
632 K., Butler, A., Kahlheber, S. (Eds.), *Food, fuel and fields: progress in African archaeobotany.*  
633 *Heinrich-Barth-Institut, Köln, Africa Praehistorica* 15, pp. 163-175.  
634  
635

636

637

638

Supplementary material 1:

We know from figure 2a that the relative error of the reconstructed diameters is really high for small angles. We tried to find a quantitative justification to set a lower limit under which the method should not be used because of too important errors.

Our first try was to identify outliers from the RE distribution as being outside 1.5 times the interquartile range above the upper quartile and below the lower quartile. The range of “normal data” was then [-0.825, 0.815]. We would then select only the data which angles are higher to the last observation being consider as outlier.

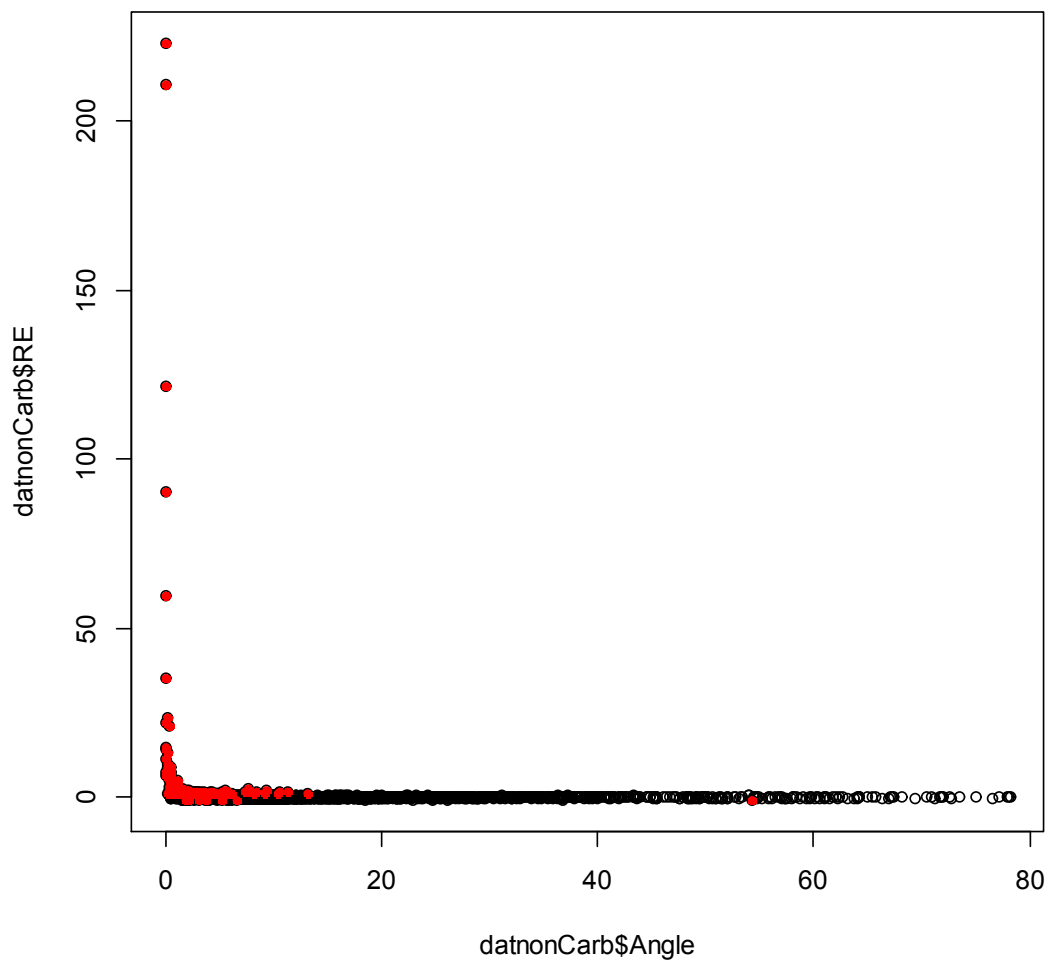


Figure SM1.1. Scatter plot of the relative errors of diameters estimations and angles. Red dots indicated data which are outside 1.5 times the interquartile range above the upper quartile and below the lower quartile { -0.825, 0.815}.

Unfortunately, an outlier appeared at an angle of 54.28 with an RE negative which was not what we expected to remove. Even by ignoring this point, the next limit was at 13.2 and we knew that linear

regression was quite good even for smaller angles. We then tried to include values inside a range of 99% around the median.

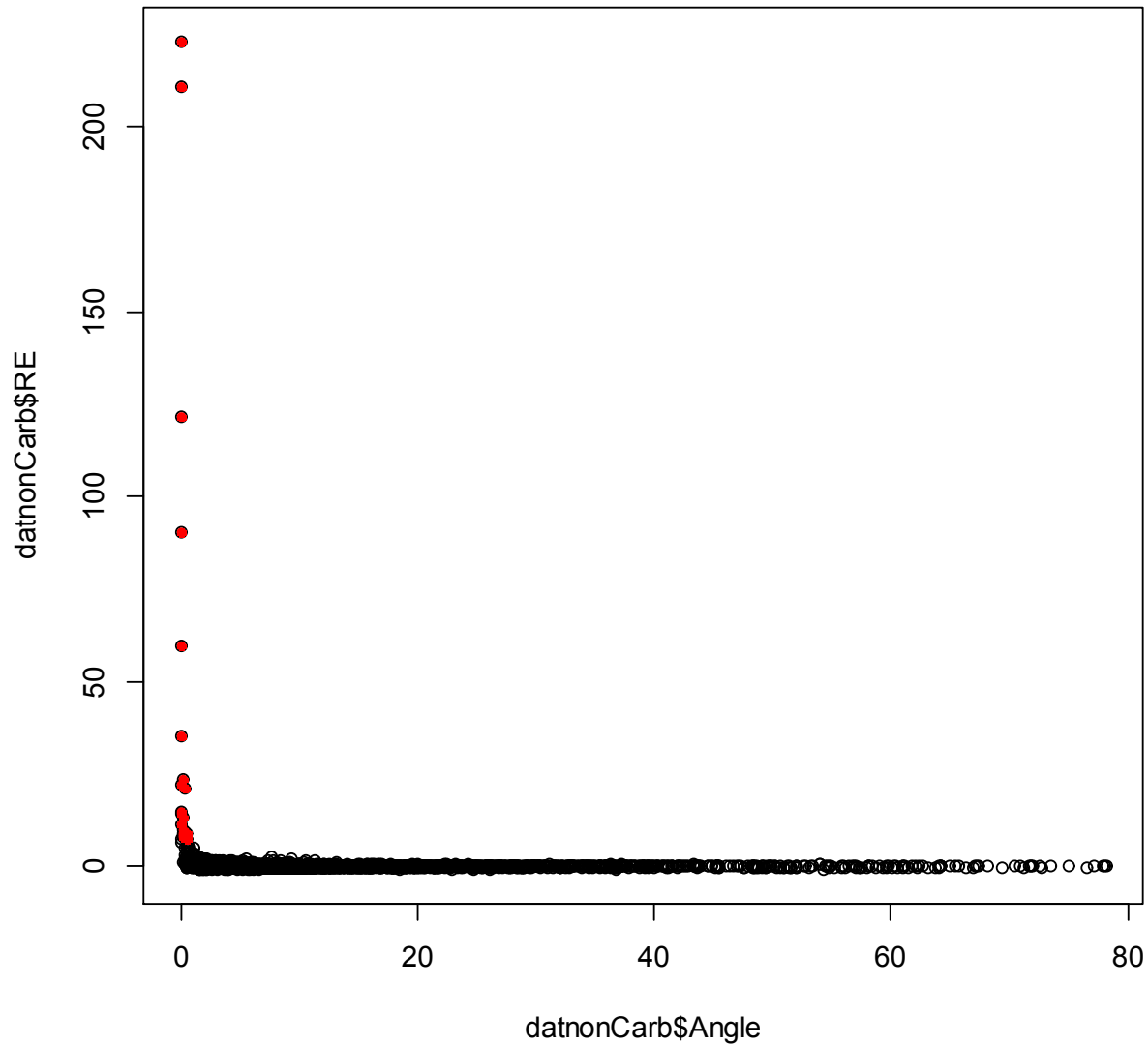


Figure SM1.2. Scatter plot of the relative errors of diameters estimations and angles. Red dots indicated data which are outside the 0.99 quantiles range  $[-0.99000, 7.50295]$ .

This time too many observations were kept and would have biased models very much at small angles. We finally considered that looking for outliers had some subjectivity in the quantile we would have selected to recognize the lower angle limit.

We then switched to Cook's distances (Cook & Weisberg, 1980) to identify points that would influence the regression too much in comparison to the others. The usual limit is 4 times the mean of the cook's distances of all the observations. This operation identifies four observations that are outside the limit (Fig. SM1.3).

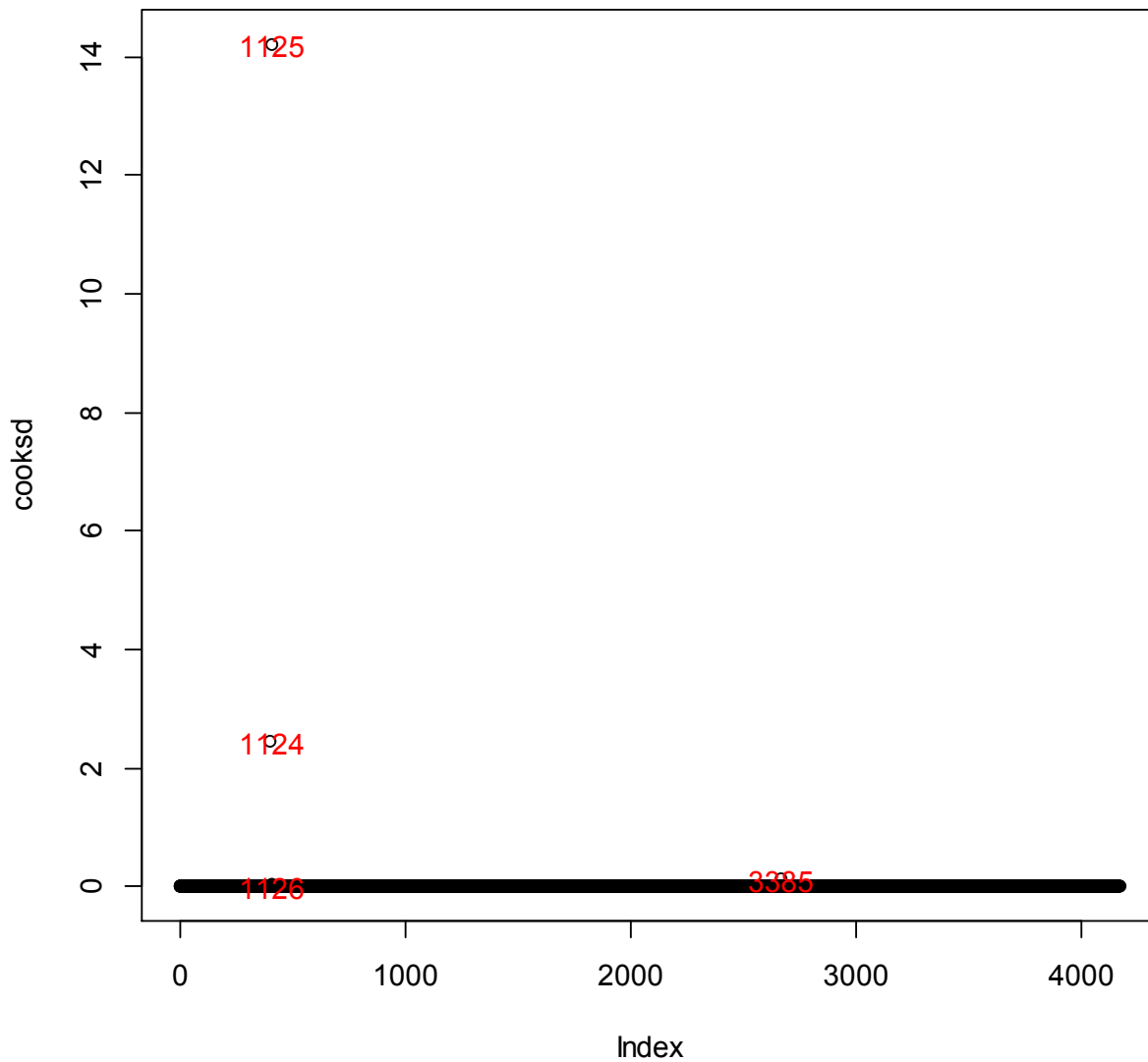


Figure SM1.3. Cook's distance of every point from the regression  $RR = a * CR + b$ .

We thus still have an important bias at small angles. We decided to try an iterative procedure by using a loop on the previous procedure and to run it until no points were outside the range. 46 runs were computed until it stabilized leaving only 983 points over the 4164 from the original dataset. This

reduction of the dataset would have too much weakens the study and the regressions would be artificially good.

We finally decided to compute moving average and dispersion intervals to recognize the point where the variability was reasonably small and the successive means centered on 0 (Fig.SM1.4, SM1.5). These two conditions are necessary to both have a good precision and resolution in our models. The value of 2 degrees appeared as the good balance between these properties and the number of points considered to build the models. We hope to find a more robust procedure in the future.

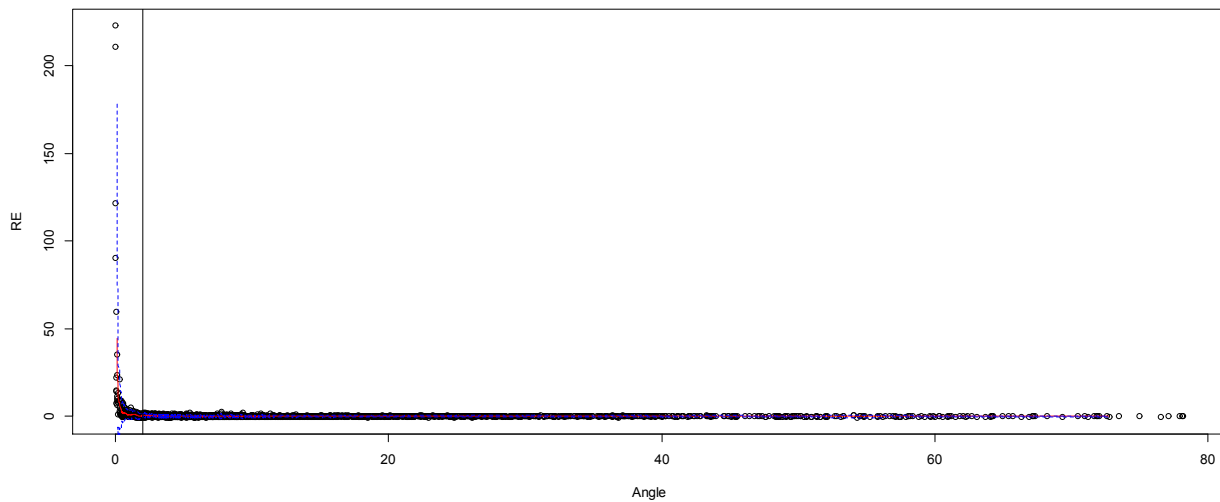


Figure SM1.4. Scatterplot of the Relative Errors and angles. Red line represents the moving average and blue dashed lines the moving average  $\pm 2$  standard deviations. Windows of 20 consecutive points. The vertical bars is angle = 2.

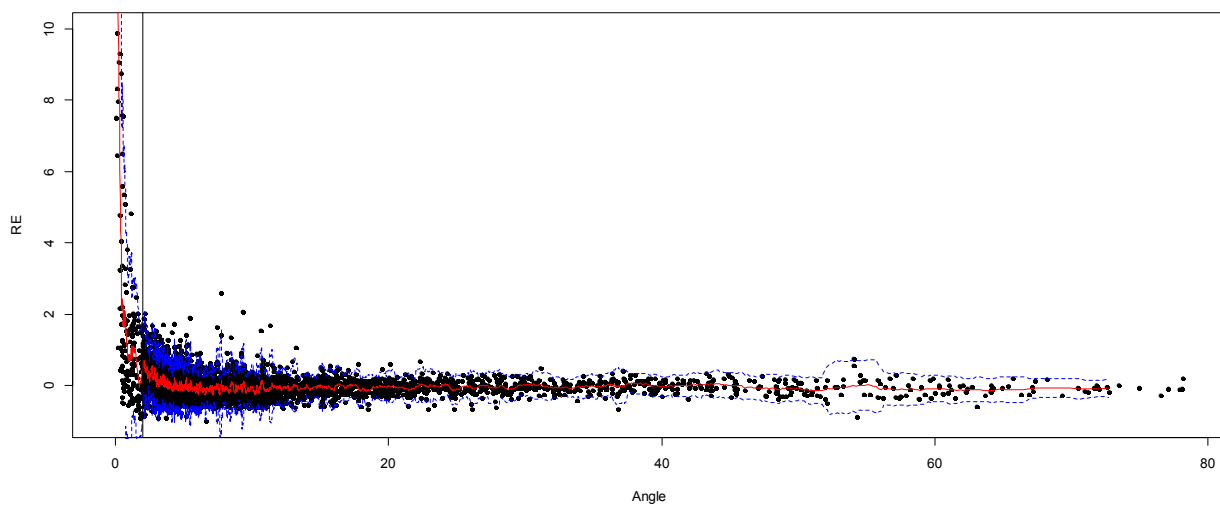


Figure SM1.5. Idem as fig.SM3.4 but limits of the y axis set to  $\{-1, 10\}$ .

## Script:

```
# a common way to identify outliers is to consider as an outlier a value which is
# outside 1.5 times the interquartile range above the upper quartile and below the
# lower quartile.
# in our example lets check the variability of RE
qu<-quantile(datnonCarb$RE)
# so the range is
rangeQ<-c(qu[2]-(1.5*(qu[4]-qu[2])),qu[4]+(1.5*(qu[4]-qu[2])))
# we can remove lines which RE is outside [-0.825 , 0.815]
datnonCarbNoOut<-datnonCarb[datnonCarb$RE<rangeQ[2]&datnonCarb$RE>rangeQ[1],]
datnonCarbOut<-datnonCarb[datnonCarb$RE>rangeQ[2]|datnonCarb$RE<rangeQ[1],]
# check graphically
plot3d(datnonCarbNoOut$Distance,datnonCarbNoOut$RE,datnonCarbNoOut$Angle)
# which angles are related to these outliers
angleIn<-datnonCarb$Angle[datnonCarb$RE<rangeQ[2]&datnonCarb$RE>rangeQ[1]]
angleOut<-datnonCarb$Angle[datnonCarb$RE>rangeQ[2]|datnonCarb$RE<rangeQ[1]]
hist(angleOut)
hist(angleIn)
# many good RE are for small angles (~1400 for {0,5})
plot(datnonCarb$Angle,datnonCarb$RE)
points(datnonCarbOut$Angle,datnonCarbOut$RE, pch= 20,col="red")
# lets say now we want 99%
rangeQ<-quantile(datnonCarb$RE, probs = c(0,0.995))
datnonCarbNoOut<-datnonCarb[datnonCarb$RE<rangeQ[2]&datnonCarb$RE>rangeQ[1],]
datnonCarbOut<-datnonCarb[datnonCarb$RE>rangeQ[2]|datnonCarb$RE<rangeQ[1],]
plot(datnonCarb$Angle,datnonCarb$RE)
points(datnonCarbOut$Angle,datnonCarbOut$RE, pch= 20,col="red")
abline(v=2)
plot(datnonCarb$Angle,datnonCarb$RC)
points(datnonCarbOut$Angle,datnonCarbOut$RC, pch= 20,col="red")
## test avec cooks distances
mod <- lm(RR~Rctrigo, data=datnonCarb)
cooksds <- cooks.distance(mod)
plot(cooksds)
abline(h = 4*mean(cooksds, na.rm=T), col="red") # add cutoff line
text(x=1:length(cooksds)+1, y=cooksds, labels=ifelse(cooksds>4*mean(cooksds, na.rm=T),names(cooksds),""), col="red") # add
labels

datnonCarbCD<-datnonCarb[cooksds<4*mean(cooksds, na.rm=T),]
plot(RR~Rctrigo, data=datnonCarbCD)
# test loop cooks distance
isCD<-0
datnonCarbCD<-datnonCarb
count<-0
while (isCD!=1) {
  mod <- lm(RR~Rctrigo, data=datnonCarbCD)
  cooksds <- cooks.distance(mod)
  datnonCarbCD<-datnonCarbCD[cooksds<4*mean(cooksds, na.rm=T),]
  if(all(cooksds<4*mean(cooksds, na.rm=T))) {isCD<-1}
  plot(RR~Rctrigo, data=datnonCarbCD)
  count<-count+1
}
plot(RR~Rctrigo, data=datnonCarb)

## moving average on RE / Angle
width<-10
meansRE<-running(datnonCarb$RE[order(datnonCarb$Angle)],fun=mean,width=width,by=1)
```

```
meansAngle<-running(datnonCarb$Angle[order(datnonCarb$Angle)],fun=mean,width=width,by=1)
sdRE<-running(datnonCarb$RE[order(datnonCarb$Angle)],fun=sd,width=width,by=1)
plot(RE~Angle, data=datnonCarb),ylim=c(-1,10),pch=20)
lines(meansAngle,meansRE,col="red")
lines(meansAngle,meansRE-2*sdRE,col="blue",lty=2)
lines(meansAngle,meansRE+2*sdRE,col="blue",lty=2)
abline(v=2)
```

#### Additional references.

Cook, R. D. and Weisberg, S. (1982). *Residuals and Influence in Regression*. London: Chapman and Hall.

## Legend

Table 1 – Number of measurements on perfect target performed with each PLT (manual and semi-automatic)

Table 2 – Number of measurements taken for each taxon. The reference number of the wood slices corresponds to that given for the dendro-anthracological reference collection, available to researchers (UMR 7209, Paris)

Table 3. Akaike Criterion Information (AIC) for the three models tested and  $R^2$  of the best one for each taxon. reg: classic regression, wreg: weighted regression, swreg: segmented weighted regression. Values in bold represents the lowest AIC (the best model) corresponding for all taxa to swreg.

Table 4. Details of the swreg model for all taxa. The first slopes (lowest CR) are very similar between taxa. Notable differences are the breakpoints. Bold values indicate p-values lower than 0.05. P-values for breakpoints and slope 2 are not currently available; we use std.error to estimate the confidence in the results. The swreg model indicates significant differences between taxa regarding the breakpoints.

Table 5. Estimations, standard errors of the parameters and  $R^2$  of the swregCarb model for *Pinus halepensis* (A) and *Fagus sylvatica* (B).

Figure 1: Kernel density of the relative errors (RE) measured on perfect targets. Comparison of manual and semi-automatic PLTs.

Figure 2: Biplots of angles between ligneous rays and relative errors (RE). A: representation of all the data, the vertical bar corresponds to an angle of  $2^\circ$  that is the threshold recommended in this paper. B: Boxplot of the data from which angles inferior to  $2^\circ$  have been removed and organized into classes.

Figure 3 – Scatter plot of the real radii (RR) over the calculated radii (CR), each panel corresponds to a taxon (fresh wood).

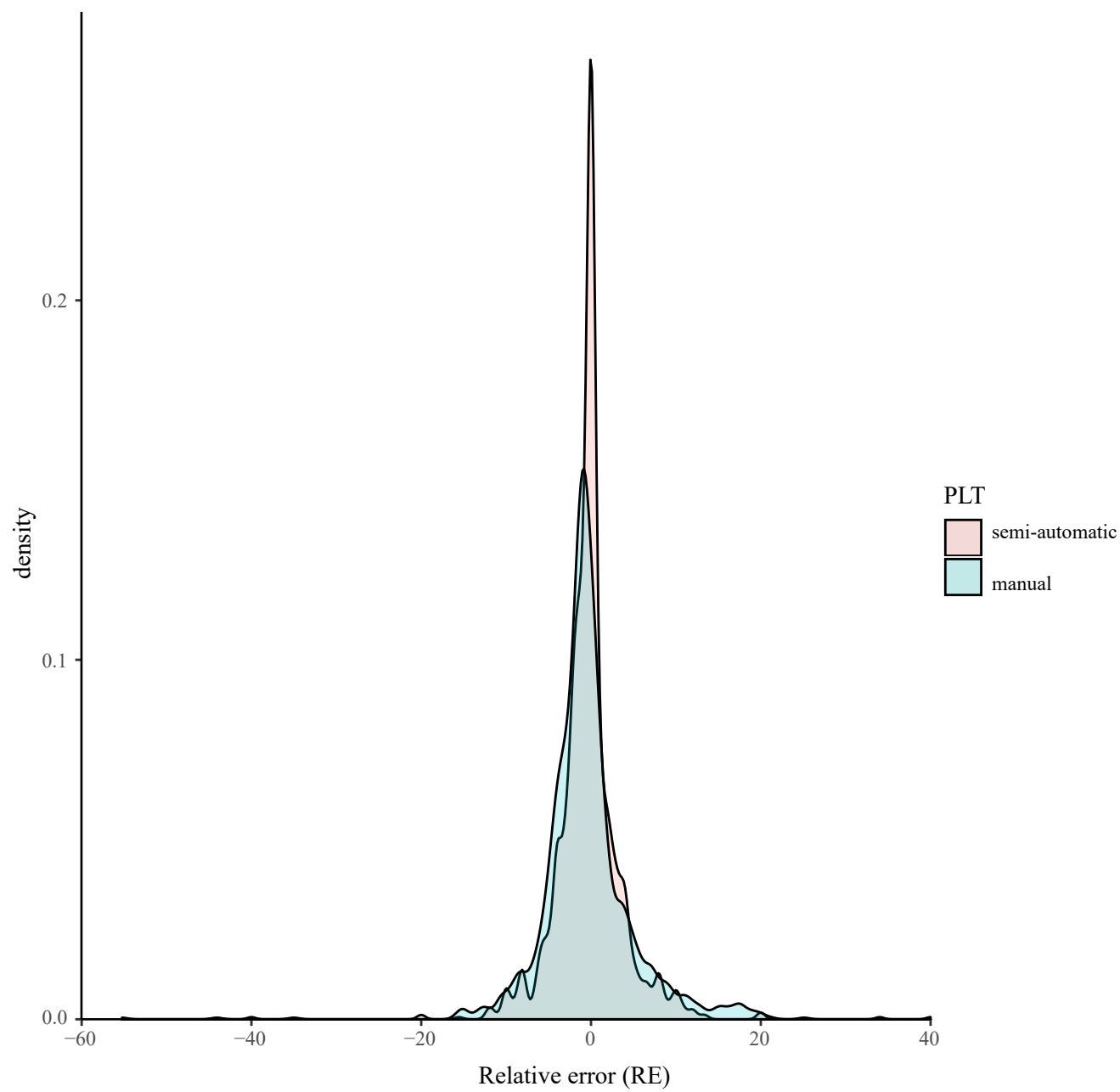
Figure 4 – Fitted lines corresponding to the swreg model for all taxa. The solid lines represent the estimation, the dashed lines represent the 0.95 prediction interval, and horizontal bars represent the 0.95 confidence interval around the estimation of the breakpoints represented by circles

Figure 5\_ Fitted lines corresponding to the swregCarb model for *Pinus halepensis* and *Fagus sylvatica* whether or not carbonized. The solid lines represent the estimation and the dashed lines represent the 0.95 prediction interval.

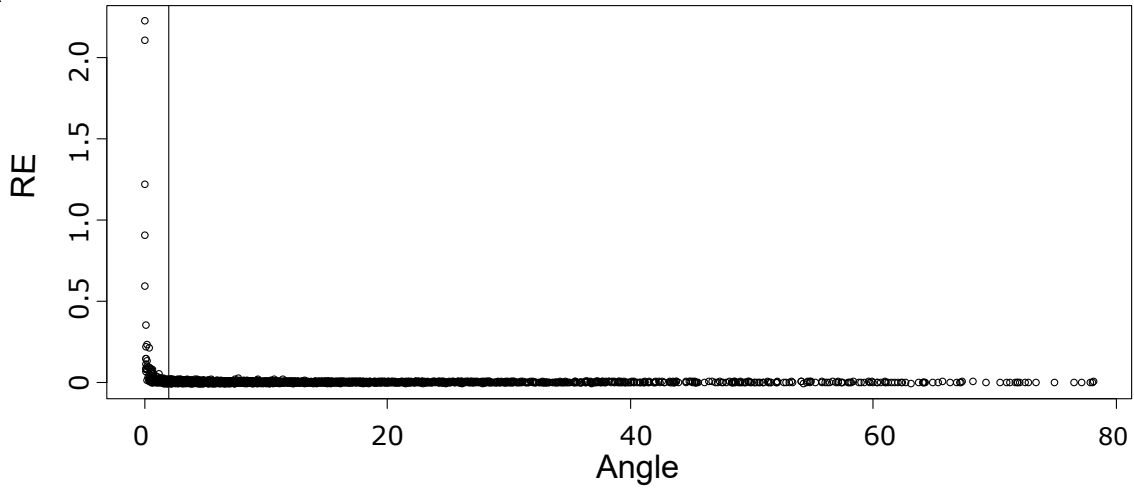
Figure 6 -a- Fresh wood of *Quercus petraea*, without tension wood. All the wood rays converge to the pith. b- Fresh wood of *Quercus petraea*, with tension wood. The direction of the rays changes to adapt to the new morphology of the wood.

SM 1 - the different statistical methods tried in order to provide the user a practical minimum angle

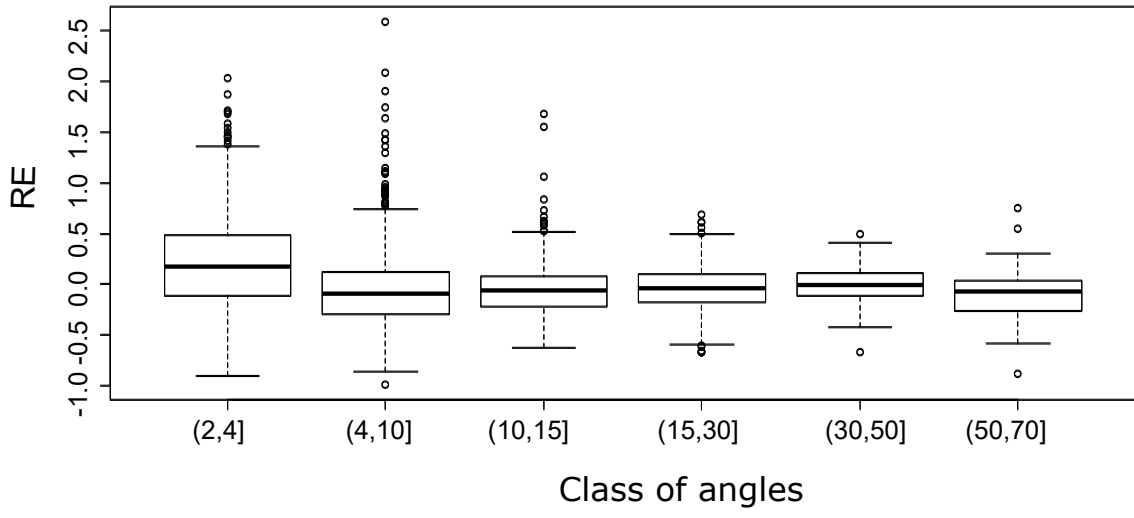
SM 2 – Boxplot of the relative errors (RE) on perfect targets depending on the distances between rays. A: Boxplot of all the data B: Boxplot of the data from which angles inferior to 2° have been removed.

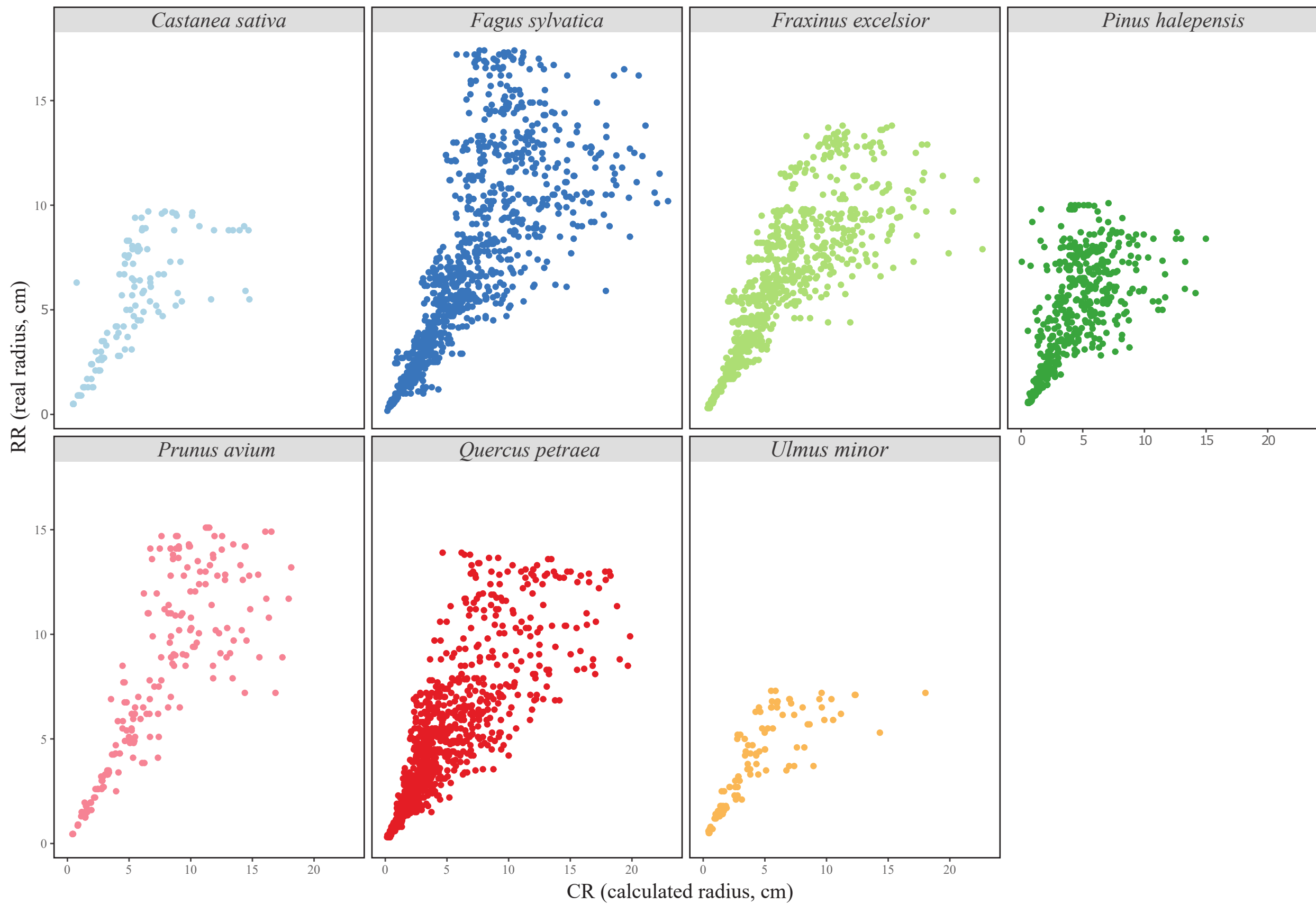


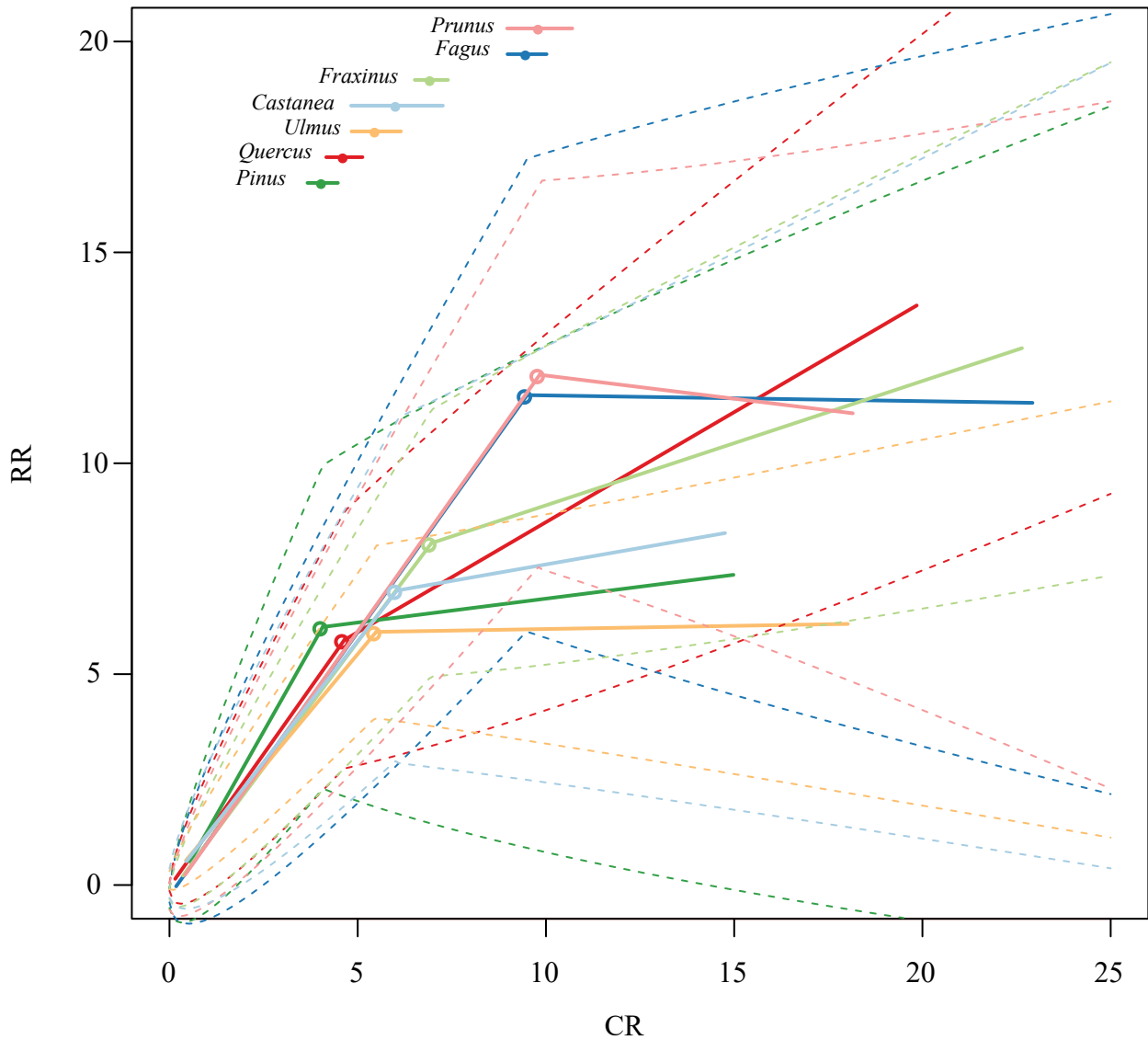
A



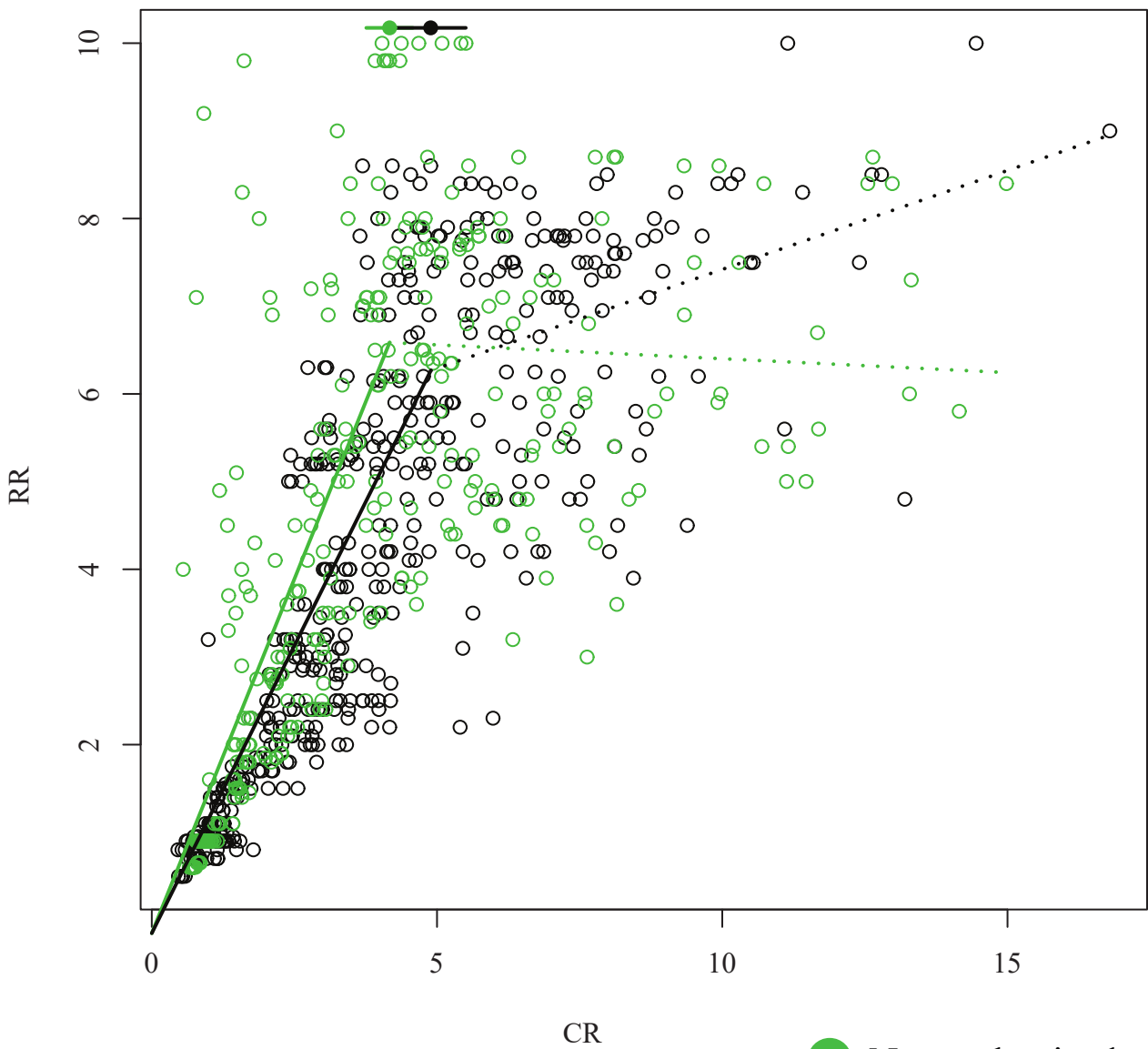
B





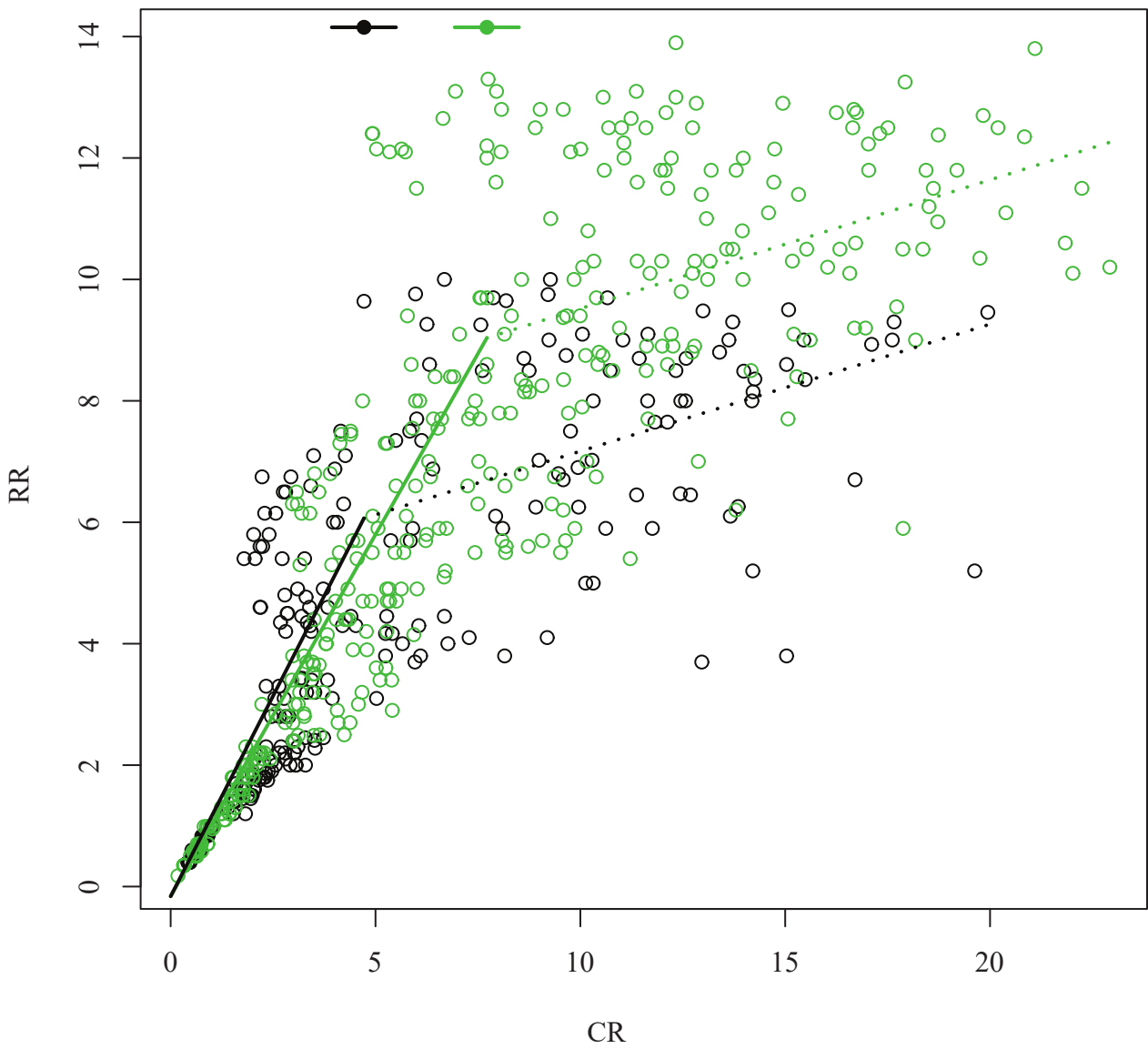


*Pinus halepensis*



- Non carbonized
- Carbonized

*Fagus sylvatica*





## Author statement

Alexa Dufraisse : Conceptualization, Methodology, Archaeological data curation  
, Writing- Original draft preparation, Supervision

Jérémie Bardin : Statistical treatment and modelisation

Llorenç Picornell-Gelabert : Archaeological data curation

Sylvie Coubray : Archaeological data curation

Maria Soledad Garcia-Martinez : modern reference data curation

Michel Lemoine : technical supervision

Sílvia Vila Moreiras : modern reference data curation